Chemical Engineering Journal 132 (2007) 227–232

Chemical Engineering Journal

www.elsevier.com/locate/cej

Simultaneous absorption of NO and SO_2 by Fe^{II}EDTA combined with Na_2SO_3 solution

Li Wang, Weirong Zhao, Zhongbiao Wu *

Department of Environmental Engineering, Zhejiang University, Hangzhou 310027, China

Received 18 August 2006; received in revised form 11 December 2006; accepted 20 December 2006

Abstract

The simultaneous absorption of NO and SO_2 by Fe^{II}EDTA combined with Na_2SO_3 solution was studied by cyclic voltammetry and Raman spectroscopy for the purpose of investigation on the reaction products and reaction mechanism. It was found that the high efficiency (more than 60%) period of NO absorption with the presence of SO_2 was 1.59 times longer than that without SO_2. At the same time, the existence of SO_2 increased the absorption capability of NO by 36.65% within 500 min, compared with NO absorption by Fe^{II}EDTA combined with Na_2SO_3 solution. The reason may be explained that part of NO had been reduced by SO_2 before entering into Fe^{II}EDTA solution combined with Na_2SO_3. The addition of Na_2SO_3 changed pH value of the solution and provided SO_3^{2-} which realized the regeneration of Fe^{II}EDTA absorption solution. The main reactions of the system included the reductions of Fe^{II}EDTA(NO), Fe^{III}EDTA and NO absorption. The majority consumed SO_3^{2-} were converted into SO_4^{2-}.

Keywords: Fe^{II}EDTA; Nitric oxide; Absorption; Mechanism

1. Introduction

NO_x and SO_2 emission from combustion of coal, fuel oils and waste have given significant effects on environment and human health. Current techniques for controlling sulfur dioxide flue gas desulfurization (FGD) include spraying or injecting slurry, for example, calcium hydroxide, or limestone as sorbents [1]. Although FGD has experienced high SO_2 removal, that is not so for NO_x. The present techniques for controlling nitrogen oxide such as selective catalytic reduction (SCR), selective non-catalytic reduction (SNCR) suffer from the problems of selectivity, high cost [2] and catalyst sulfur poison by residual SO_2 in FGD [3]. Wet process of NO_x by adding some additives to improve NO water solubility is a competitive method since it may realize simultaneous removal of SO_2 [4–6].

The absorption of NO_x by means of complexes is a method by which metal complex solutions react with the absorbed NO to form metal-nitrosyl complexes rapidly [7]. However, the common metal complex solution Fe^{II}EDTA can be easily oxidized to Fe^{III}EDTA species and loses the ability to bind NO. As a consequence the regeneration of absorption solution becomes a fundamental part of this method. Various reducing agents such as Na_2SO_3 [8], $Na_2S_2O_4$ [9], hydrazine [10] and certain polyphenolic compounds [11] had been tested and their regenerations proved to be effective. Among these reducing agents, the extensively examined reducing agents for the regeneration of Fe^{III}EDTA solution were sulfite ion (SO_3^{2-}) and bisulfite ion (HSO_3^-) [12,13]. Although it was highly desirable for SO_3^{2-} converted from SO_2 to be capable of regenerating Fe^{II}, the results showed that this process depended on pH value [13]. Na_2SO_3 was added into the Fe^{II}EDTA solution and many attentions (Sada et al. [8]; Narita et al. [14]) had been paid on simultaneous absorption of NO and SO_2 by Fe^{II}EDTA combined with Na_2SO_3, since Na_2SO_3 was one of the ingredients in dual-alkali process which had been used to absorb SO_2. It was found that the coexisting SO_2 played a part in releasing SO_3^{2-} from the complex Fe^{II}EDTA (SO_3^{2-})(NO) formed in the absorption, and the presence of SO_2 in the gas phase effectively improved pH value of the solution toward favorable values for the reaction of NO with Fe^{II}EDTA. The absorption rate of NO in the presence of SO_2 tended to decrease with increasing SO_2 concentration [12]. The absorption was so complicated that various analytical methods, such as gas chromatography, mass spectrometry and Raman spectroscopy, were applied to study this process.

---

* Corresponding author. Tel.: +86 571 8795 2459; fax: +86 571 8795 3088.
E-mail address: zbwu@zju.edu.cn (Z. Wu).

1385-8947/$ – see front matter © 2007 Elsevier B.V. All rights reserved.
doi:10.1016/j.cej.2006.12.030

Apart from the oxidation of $Fe^{II}EDTA$ and reduction of NO, the observed reaction products were $SO_4{}^{2-}$, $S_2O_6{}^{2-}$ and some N–S compound such as $HON(SO_3)_2{}^{2-}$ [8,13] and $(NO)_2SO_3{}^{2-}$ [15,16].

In this paper, simultaneous absorption of NO and low concentration SO_2 was undergone with the aim of exploring the influences of SO_2 on NO absorption, in addition, cyclic voltammetry [17,18], which has been receiving considerable interests due to its importance for providing desirable features on electron transfers, was applied to simulate chemical reaction process and analyze reaction mechanism.

2. Experimental

2.1. Experimental set-up

The experimental set-up is shown in Fig. 1. The experiment was performed in a double-stirred vessel with 76 mm diameter and 150 mm height. Both gas phase and liquid phase were stirred by four stainless steel impellers. Four baffles of 129 mm (height) × 5 mm (width) were used to assist mixing. The double-stirred vessel had a water jacket through which water was circulated to control the temperature in the reactor.

The absorption of NO was carried out in 0.01 M $Fe^{II}EDTA$ solution at 303 K. NO and SO_2 were diluted by N_2 to the desired concentrations in mixing vessel before being fed to the double-stirred vessel. The inlet concentration of NO was in the range of 400–500 ppm. The 100 ppm SO_2 was blown into the mixing vessel to investigate its effects on absorption. The continuous total gas flow rate was maintained at 6 ml s^{-1}.

The complex solution of $Fe^{II}EDTA$ was prepared by adding equimolar amount of $FeSO_4$ and Na_2EDTA to deionized water. The initial pH value of the solution was adjusted by NaOH or HCl. The measurement of pH value was performed by acidimeter (Rex, Shanghai).

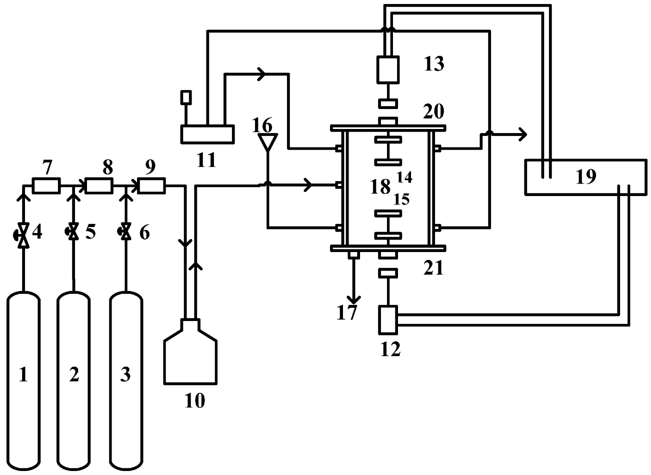

Fig. 1. Schematic diagram of experimental apparatus: 1, N_2 gas cylinder; 2, NO gas cylinder; 3, SO_2 gas cylinder; 4–6, relief valves; 7–9, gas flow meters; 10, mixing vessel; 11, thermostat; 12 and 13, driving motors; 14 and 15, stirrers; 16, absorption solution inlet; 17, absorption solution outlet; 18, double-stirred vessel; 19, voltage stabilized power; 20 and 21, magnetic drives.

2.2. Analysis methods

The concentration of NO was analyzed by Griess Saltzman method. NO was firstly oxidized to NO_2 by CrO_3 powder filled in glass tube. The oxidized gas was absorbed by Griess Saltzman solution (containing 50 ml glacial acetic acid, 5.0 g sulfanilic acid and 50 mg *N*-1-naphthylethylenediamine dihydrochloride (NEDH) per 1000 ml solution) to form $NO_2{}^-$. The latter reacted with sulfanilic acid to form a diazoimido compound, and then coupled with NEDH to produce a red-violet azo compound in 15 min. Finally, the concentration was determined by spectrophotometer 722S (Lengguang Tech., China) at the band of 540 nm [19].

In the case of the present system, gas flow rate and NO inlet concentration were previously known. Absorption capability for a fixed period of time could be achieved by graphical integration under the curves of removal of NO in absorption solution [8].

Electrochemical measurements were performed by Potentiostat/Galvanostat (EG & G Model 273A) in a three-electrode glass cell. The reference electrode was a saturated calomel electrode (SCE) with a luggin capillary probe placed near the working electrode surface to minimize the ohmic drop through the cell. Both the working electrode with area 1.02 cm^2 and the counter electrode were platinum foil. Deaeration of the test solution was achieved by bubbling pure nitrogen for 30 min before use. Without special specification, all the potentials were relative to SCE.

The species in solution were studied by ion chromatogram (Dionex ICS-90) and classical chemical analysis [20] on account of their accuracy and convenience. Raman spectroscopy (Almega Dispersive Raman, Thermo Nicolet Co.) was used to detect the existences of $S_2O_6{}^{2-}$ [13], $HON(SO_3)_2{}^{2-}$ [13], $S_2O_4{}^{2-}$ [21] and $S_2O_3{}^{2-}$ [21]. The decomposition of EDTA was studied by mass spectrometry (Bruker Esquire 3000 plus). The absorption and determination tests were all carried out under the anoxic condition.

3. Results and discussion

3.1. Absorption analyses

pH value is a crucial parameter in NO absorption by $Fe^{II}EDTA$ solution [8]. The absorption of NO by $Fe^{II}EDTA$ solution was firstly studied in double-stirred vessel to find the optimum pH value for absorption. Fig. 2 shows that NO absorption capabilities are 17.06, 15.75 and 14.18 ml, respectively, within 165 min at pH values 8, 7 and 5. In weak alkaline solution more NO was absorbed. The absorption capability of NO by $Fe^{II}EDTA$ solution at pH value 8 was optimum.

Strong acid or alkaline solution is not suitable for NO absorption because $Fe^{II}EDTA$ can be easily oxidized in strong acid solution according to

$$2NO + 2Fe^{II}EDTA + 2H^+ \rightarrow N_2O + 2Fe^{III}EDTA + H_2O \quad (1)$$

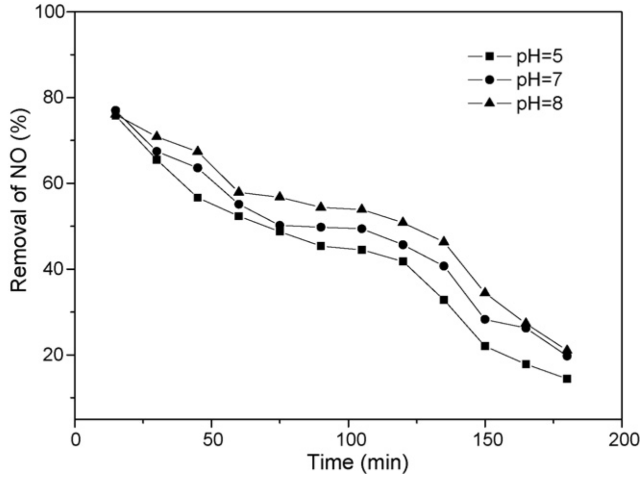

Fig. 2. Absorption of NO by $Fe^{II}EDTA$ solution at different pH. $C_{Fe^{II}EDTA} = 0.01$ M, $C_{NO} = 500$ ppm, $T = 303$ K.

While in alkaline solution $Fe^{II}EDTA$ is not stable enough because of the precipitation of Fe^{2+}

$$Fe^{2+} + OH^- = Fe(OH)_2 \tag{2}$$

When NO dissolves in water

$$NO + NO_2 + H_2O = 2HNO_2 \tag{3}$$

The formed HNO_2 easily dissolves in weak alkaline solution and promotes NO absorption.

Fig. 3 shows the absorption comparison after the addition of 0.25 M Na_2SO_3 into 0.01 M $Fe^{II}EDTA$ solution. At pH value 8 the absorption capability for NO by $Fe^{II}EDTA$ solution was 18.24 ml within 280 min. While absorption capabilities for NO by $Fe^{II}EDTA$ solution combined with Na_2SO_3 were 34.69 ml within 280 min and 47.12 ml within 500 min. The addition of Na_2SO_3 into $Fe^{II}EDTA$ solution enhanced NO absorption capability by 90.19% within 280 min. This may be explained as the reduction of $Fe^{II}EDTA(NO)$ by Na_2SO_3 according to the following reactions [13]:

$$2Fe^{II}EDTA(NO) + SO_3{}^{2-} = 2Fe^{II}EDTA + (NO)_2SO_3{}^{2-} \tag{4}$$

$$(NO)_2SO_3{}^{2-} = N_2O + SO_4{}^{2-} \tag{5}$$

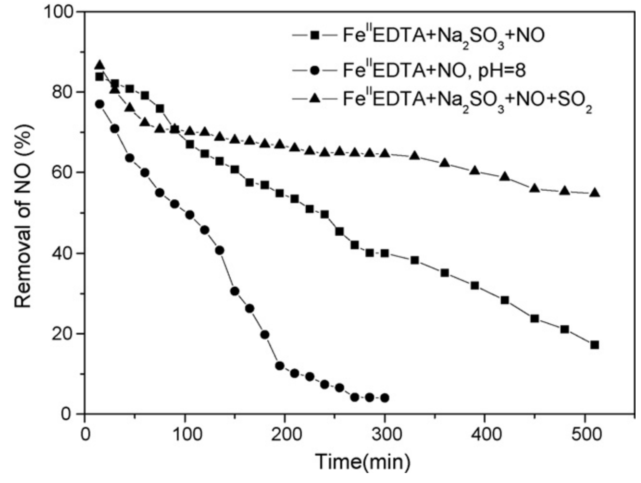

Fig. 3. Time dependence of removal of NO in $Fe^{II}EDTA$ solution and $Fe^{II}EDTA$ combined with Na_2SO_3 solution. $C_{Fe^{II}EDTA} = 0.01$ M, $C_{Na_2SO_3} = 0.25$ M, $C_{SO_2} = 100$ ppm, $C_{NO} = 500$ ppm, pH 8, $T = 303$ K.

Absorption capability of NO in the presence of SO_2 was 64.39 ml within 500 min. The simultaneous existence of SO_2 increased the absorption capability of NO by 36.65% within 500 min. NO removal efficiency was more than 55% within 500 min. The reason that coexisting 100 ppm SO_2 increased absorption capability may be explained as

$$2NO + SO_2 = N_2O + SO_3 \tag{6}$$

Gibbs energy $\Delta G_m^0 = -139.8$kJ/mol. Equilibrium constant is 2.86×10^{24}. $\Delta_r H_m^0 = -197.3$kJ/mol. Exothermal reaction (6) easily takes place at lower temperature. This indicates that some NO has been reduced before entering into solution. The presence of low concentration of SO_2 did not take great effect on pH value. pH value remained 8 after 100 ppm SO_2 was bubbled into $Fe^{II}EDTA$ solution combined with Na_2SO_3. The remained NO was absorbed by solution and Na_2SO_3 reduced $Fe^{II}EDTA(NO)$ and $Fe^{III}EDTA$. According to Fig. 3, it could be calculated that the high efficiency (more than 60%) period of NO absorption with the presence of SO_2 was 1.59 times longer than that without SO_2, and the decrease of NO absorption rate was slowed down.

3.2. Reaction products and mechanism

3.2.1. Discerning the reaction products

Cyclic voltammetry was used to explore electrochemical behaviors of $Fe^{II}EDTA$ solution, $Fe^{II}EDTA(NO)$ solution and Na_2SO_3 solution, respectively, in order to discern the reaction products and mechanism.

3.2.1.1. Fates of reactants. The cyclic voltammetry was used to determine the possible reactant conversions of $Fe^{II}EDTA$, NO and Na_2SO_3. Fig. 4(a and b) illustrates the conversions of $Fe^{II}EDTA$ and $Fe^{II}EDTA(NO)$ solution. The forward one half-cycle of Fig. 4a consists of an initial region of hydrogen evolution followed by one anodic peak A (−0.05 V). By reversing the potential direction after oxygen evolution, the backward one half-cycle of the voltammogram is obtained with corresponding cathodic peak B (−0.206 V) observed. Ogura and Ozeki [22] also found that the anodic peak and cathodic peak were around −0.05 and −0.20 V, respectively. They were assignable to the oxidation and reduction reactions of $Fe^{II}EDTA$. In this simple system the redox reaction may be written as:

$$Fe^{III}EDTA + e^- = Fe^{II}EDTA \tag{7}$$

NO was bubbled in $Fe^{II}EDTA$ solution for about 120 min and then the produced $Fe^{II}EDTA$ (NO) was analyzed. Fig. 4b illustrates that the anodic peak C (+0.95 V) appears after peak E (−0.03 V). By reversing the direction of potential after oxygen evolution, a cathodic peak D (+0.1 V) is observed. The anodic

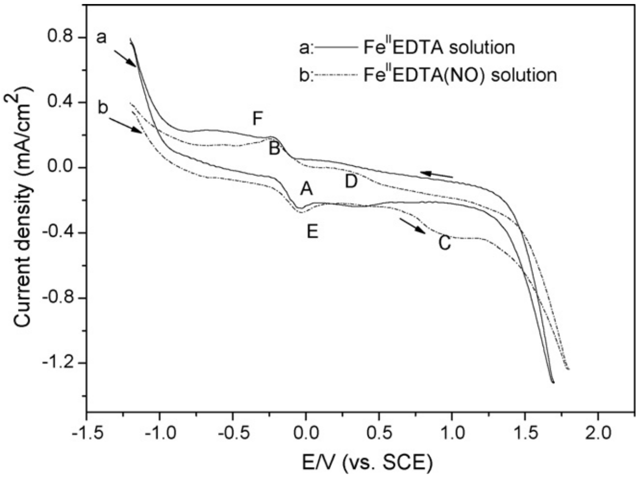

Fig. 4. Cyclic voltammograms for Fe^{II}EDTA and Fe^{II}EDTA(NO) solution. $C_{Fe^{II}EDTA} = 0.01$ M, pH 8, scan rate = 5 mV s^{-1}, $T = 303$ K.

peak C around 0.9 V, which was considered as related to the oxidation of Fe^{II}EDTA(NO) [22], can be attributed to the formation of NO_3^- according to reaction (8):

$$NO_3^- + 4H^+ + 3e^- = NO + 2H_2O \tag{8}$$

Ion chromatogram confirmed the existence of NO_3^-. The cathodic peak D is connected with the reduction of NO. It might be the formation of NH_4^+, N_2 or N_2O. NaOH was dripped and the solution was heated. Wet litmus test paper remained unchanged, indicating no NH_4^+ formation. N_2 is a minor reaction product whose production is at very high pH condition [13]. Its reduction potential is so high that it cannot be formed in this system. According to potential, the only product corresponding to peak D is the formation of N_2O

$$2Fe^{II}EDTA(NO) + 2H^+ + 2e^- = H_2O + N_2O + 2Fe^{II}EDTA \tag{9}$$

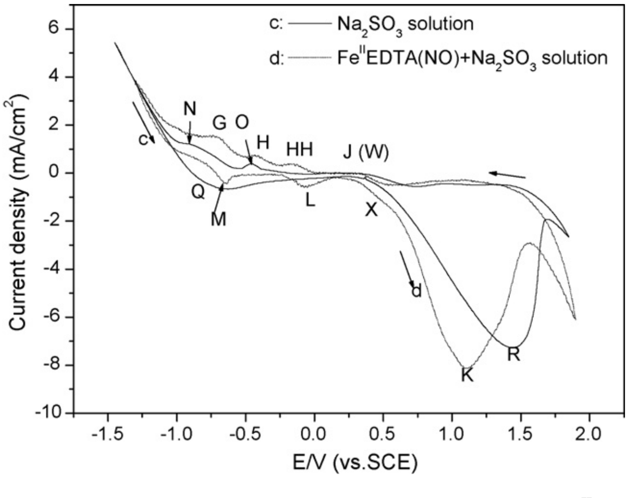

Fig. 5. Cyclic voltammograms for Na_2SO_3 and NO absorption by Fe^{II}EDTA combined with Na_2SO_3 solution. $C_{Fe^{II}EDTA} = 0.01$ M, $C_{Na_2SO_3} = 0.25$ M, scan rate = 5 mV s^{-1}, $T = 303$ K.

Fig. 5(c and d) shows Na_2SO_3 conversion and confirms SO_3^{2-} fates. Fig. 5c consists of an initial region of hydrogen evolution followed by two anodic peaks Q (−0.75 V) and R (+1.4 V) before oxygen evolution. By reversing the potential direction, the backward one half-cycle of the voltammogram is obtained. It exhibits three successive well-defined cathodic peaks J (+0.1 V), O (−0.4 V) and N (−0.90 V). The anodic peak Q may be attributed to the formation of $S_2O_6^{2-}$:

$$S_2O_6^{2-} + 2e^- = 2SO_3^{2-} \tag{10}$$

The anodic peak R is observed in the potential range from 1.25 to 1.5 V, in which a higher valency oxide forms. It is also indicative of a high concentration since the peak R is large when compared with other peaks. SO_4^{2-} is electrochemically stable and can hardly be reduced at electrode surface. R may be attributed to the formation of SO_4^{2-}. Ion chromatogram confirmed the existence of SO_4^{2-}. The cathodic peaks J, O and N may be attributed to the other formations of sulfur elements such as $S_2O_3^{2-}$, S, $S_2O_4^{2-}$, etc.

3.2.1.2. Products analyses of absorption. NO was bubbled in Fe^{II}EDTA combined with Na_2SO_3 solution for 120 min and then the solution was analyzed. Fig. 5d shows the electrochemical analyses of the NO absorption by Fe^{II}EDTA and Na_2SO_3 solution. Compare Fig. 5c with d, the anodic peak X, M and K can be attributed to the generations of NO_3^-, $S_2O_6^{2-}$ and SO_4^{2-}. The anodic peak L and cathodic HH can be explained as the conversions of Fe^{III}EDTA and Fe^{II}EDTA according to reaction (7). At the position of peak W, besides reaction (9), N–S compound $(NO)_2SO_3^{2-}$ was formed according to reactions (4) and (5). J and W are almost at the same position. $AgNO_3$ and HNO_3 solution were dripped into the absorption solution to determine the existence of $S_2O_3^{2-}$. The clear solution indicated no existence of $S_2O_3^{2-}$. Ion chromatogram confirmed this point. The cathodic peaks H and G may be attributed to the formations of S and $S_2O_4^{2-}$.

NO and SO_2 were bubbled simultaneously for 120 min and Fig. 6 displays the cyclic voltammogram. The responsible reactions may involve reactions (7)–(10) and products SO_4^{2-}, $S_2O_3^{2-}$ and $S_2O_4^{2-}$. The appearance of yellow precipitation after addition of $AgNO_3$ and HNO_3 solution confirmed the existence of $S_2O_3^{2-}$ at peak WW. The reason for no cathodic peak corresponding to sulfur may be explained as the remained SO_3^{2-} in solution reacted with colloid sulfur:

$$SO_3^{2-} + S = S_2O_3^{2-} \tag{11}$$

3.2.1.3. Raman spectroscopy determination. Raman spectroscopy was used to determine the ions in solution after cyclic voltammetry scan. It confirmed the existences of SO_4^{2-}, SO_3^{2-}, $S_2O_6^{2-}$, $S_2O_3^{2-}$ and $HON(SO_3)_2^{2-}$. The results are shown in Fig. 7. The outstanding peak at 973 cm^{-1} corresponded to SO_4^{2-}. Meanwhile, the small peaks at 615(w), 628(m), 1130(w) and 1150(w) cm^{-1} (w, s and m indicate weak, strong and medium peak, respectively) were also the characteristics of the SO_4^-. SO_3^{2-} could be distinguished at the bands of 643(w) and 994(s) cm^{-1}. $S_2O_6^{2-}$ was observed at 1097(s), 706(m)

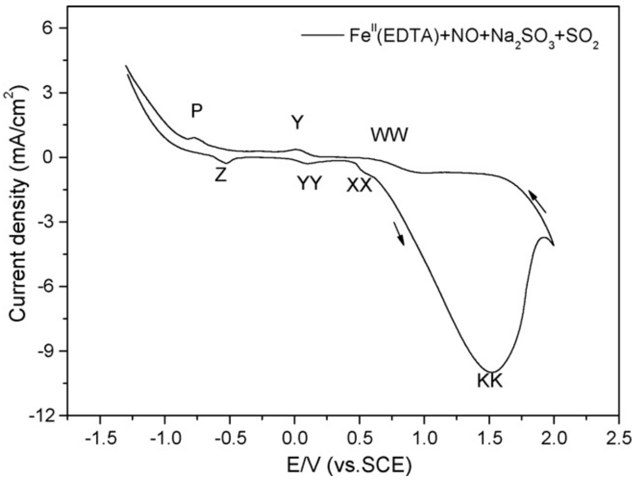

Fig. 6. Cyclic voltammogram for simultaneous absorption of NO and SO_2 by Fe^{II}EDTA combined with Na_2SO_3 solution. $C_{\mathrm{Fe^{II}EDTA}} = 0.01\,\mathrm{M}$, $C_{\mathrm{Na_2SO_3}} = 0.25\,\mathrm{M}$, scan rate = 5 mV s^{-1}, $T = 303$ K.

and 1216(m) cm^{-1}. The existence of $S_2O_3{}^{2-}$ was identified at 673(w) and 1161(w) cm^{-1}. $NO_3{}^-$ could be distinguished at the bands of 725(w) and 1069(s) cm^{-1}. $NO_2{}^-$ could be observed at the band of 827(m) cm^{-1}. The band at 1081 cm^{-1} could be attributed to $HON(SO_3)_2{}^{2-}$. Cyclic voltammogram did not suggest its existence. Its formation may be explained as the bisulfite ion ($HSO_3{}^-$) from dissolved SO_2 reacts with the formed N–S compounds such as $NOSO_3{}^{2-}$ [23]:

$$HSO_3{}^- + NOSO_3{}^- = HON(SO_3)_2{}^{2-} \qquad (12)$$

3.2.1.4. Final products. NO and SO_2 were bubbled simultaneously for 500 min. Fig. 8 shows the cyclic voltammogram of this long time absorption. The anodic peaks V and U, two cathodic peaks T and S may be attributable to the formations of $S_2O_6{}^{2-}$, Fe^{III}EDTA, Fe^{II}EDTA and $S_2O_4{}^2$. The giant peak KK disappeared indicating that most oxides of sulfur were converted into $SO_4{}^{2-}$. $BaCl_2$ and HCl solutions were applied to test the existences of $SO_4{}^{2-}$ and $SO_3{}^{2-}$. Some undissolved white precipitation and some dissolved white precipitation with acid smell confirmed their existences. Some products of the anodic decomposition of EDTA, such as formaldehyde, iminodiacetic acid, etc. could be identified by Johnson et al. [24]. However, these products were not detected by mass spectrometry in our experiment.

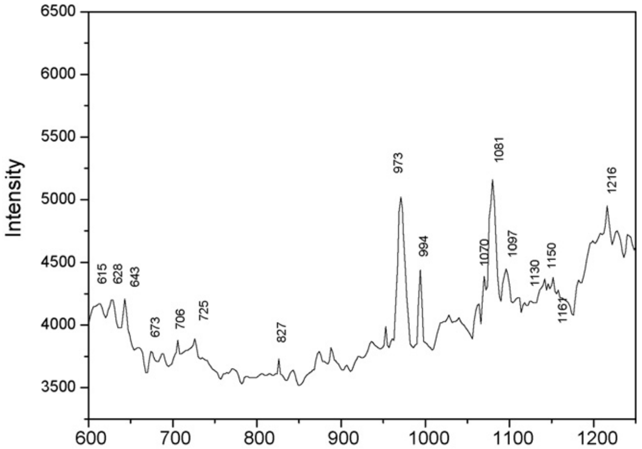

Fig. 7. Raman spectra of NO and SO_2 absorption (pH 8).

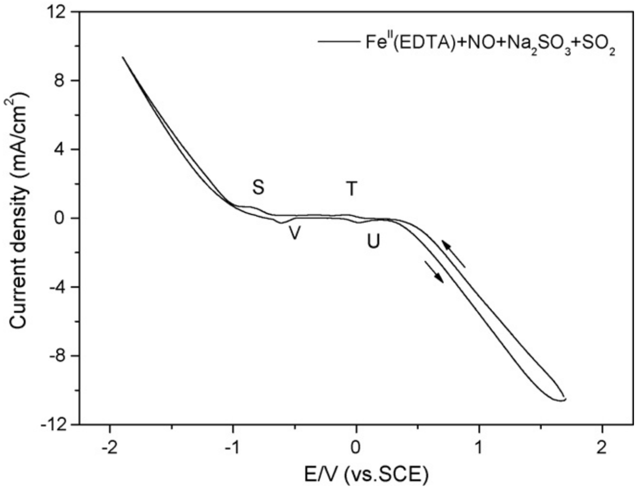

Fig. 8. Cyclic voltammogram for long time absorption of NO and SO_2 by Fe^{II}EDTA combined with Na_2SO_3 solution. $C_{\mathrm{Fe^{II}EDTA}} = 0.01\,\mathrm{M}$, $C_{\mathrm{Na_2SO_3}} = 0.25\,\mathrm{M}$, scan rate = 5 mV s^{-1}, $T = 303$ K.

3.2.2. Mechanism studies on reactions

Through, the thermodynamic calculation of equilibrium constants at pH 8, we obtain ln K for $SO_3{}^2$ conversions into $S_2O_3{}^{2-}$, S and $S_2O_4{}^{2-}$ as −6.016, −11.43 and −15.26, respectively, which indicate that the quantities of these spontaneous conversions in solution are few. Moreover, the reduction abilities of $S_2O_4{}^{2-}$ and $S_2O_3{}^{2-}$ are stronger than that of $SO_3{}^{2-}$. The formation of $S_2O_4{}^{2-}$ can only be realized on electrode at very negative potential. Potential scan helps the formations of $S_2O_4{}^{2-}$, $S_2O_3{}^{2-}$ and S on electrode. The majority of $SO_3{}^{2-}$ were consumed to reduce the complexes Fe^{II}EDTA(NO) and Fe^{III}EDTA, which were also the main reactions in the absorption. The final form of S^{IV} was $SO_4{}^{2-}$. The coordinated NO in Fe^{II}EDTA(NO) was reduced to N_2O. Besides, some nitrogen–sulfur compounds were also found accompanying the absorption. Mechanism studies on reactions are shown in Fig. 9.

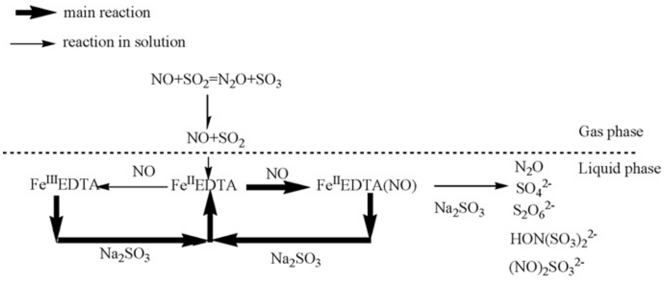

Fig. 9. Proposed mechanism on reactions. $C_{NO} = 500$ ppm, $C_{SO_2} = 100$ ppm, pH 8, $T = 303$ K.

4. Conclusion

(1) In the process of simultaneous absorption of NO and SO_2, the presence of SO_2 greatly prolonged the high efficiency (more than 60%) period of NO absorption by 1.59 times and increased the absorption capability of NO by 36.65% within 500 min. The reason may be explained as part of NO has been reduced by SO_2 before entering into Fe^{II}EDTA solution combined with Na_2SO_3.

(2) The addition of Na_2SO_3 adjusted pH value of the solution to the optimum for absorption and provided $SO_3{}^{2-}$ which regenerated the absorption solution. The main reactions in the system were the reductions of Fe^{II}EDTA(NO), Fe^{III}EDTA and NO absorption. The majority consumed $SO_3{}^{2-}$ were converted into $SO_4{}^{2-}$. The coordinated NO in Fe^{II}EDTA(NO) was reduced to N_2O.

Acknowledgments

The technical assistance and helpful discussion with Mr. J.B. Wang are gratefully acknowledged. This work is supported by New Century Excellent Human Resource Training Project of Ministry of Education (NCET04-0549) and the authors also gratefully acknowledge the financial support of Zhejiang Science and Technology Foundation (2004C23028).

References

[1] A. Garea, J.A. Marques, A. Irabien, Modelling of in-duct desulfurization reactors, Chem. Eng. J. 107 (2005) 119–125.

[2] N.A.S. Amin, C.M. Chong, SCR of NO with C_3H_6 in the presence of excess O_2 over Cu/Ag/CeO_2-ZrO_2 catalyst, Chem. Eng. J. 113 (2005) 13–25.

[3] J.D. Wang, C.Q. Wu, J.M. Chen, H.J. Zhang, Denitrification removal of nitric oxide in a rotating drum biofilter, Chem. Eng. J. 121 (2006) 45–49.

[4] S.M. Petrissans, A. Zoulalian, Influence of the pH on the interactions between nitrite and sulfite ions. Kinetic of the reaction at pH 4 and 5, Ind. Eng. Chem. Res. 40 (2001) 6068–6072.

[5] D.-S. Jin, B.-R. Deshwal, Y.-S. Park, H.-K. Lee, Simultaneous removal of SO_2 and NO by wet scrubbing using aqueous chlorine dioxide solution, J. Hazard. Mater. 135 (2006) 412–417.

[6] T.-W. Chien, H. Chu, Removal of SO_2 and NO from flue gas by wet scrubbing using an aqueous $NaClO_2$ solution, J. Hazard. Mater. 80 (2000) 43–57.

[7] T. Schneppensieper, S. Finkler, A. Czap, R. van Eldik, M. Heus, P. Nieuwenhuizen, C. Wreesmann, W. Abma, Tuning the reversible binding of NO to iron(II) aminocarboxylate and related complexes in aqueous solution, Eur. J. Inorg. Chem. (2001) 491–501.

[8] E. Sada, H. Kumazawa, Y. Takada, Chemical reactions accompanying absorption of NO into aqueous mixed solutions of Fe(II)-EDTA and sodium sulfite, Ind. Eng. Chem. Fundam. 23 (1984) 60–64.

[9] T.T. Suchecki, B. Mathews, H. Kumazawa, Kinetic study of ambient-temperature reduction of Fe^{III}edta by $Na_2S_2O_4$, Ind. Eng. Chem. Res. 44 (2005) 4249–4253.

[10] T.T. Suchecki, H. Kumazawa, Application of hydrazine to regeneration of post-absorption solutions in combined SO_2/NO_x removal from flue gases by a complex method, Sep. Technol. (1994) 763–770.

[11] M.H. Mendelsohn, J.B.L. Harkness, Enhanced flue-gas denitrification using ferrous-EDTA and a polyphenolic compound in an aqueous scrubber system, Energy Fuels 5 (1991) 244–248.

[12] E. Sada, H. Kumazawa, I. Kudo, T. Kondo, Individual and simultaneous absorption of dilute NO and SO_2 in aqueous slurries of $MgSO_3$ with Fe^{II}-EDTA, Ind. Eng. Chem. Process Des. Dev. 19 (1980) 377–382.

[13] D. Littlejohn, S.G. Chang, Reaction of ferrous chelate nitrosyl complexes with sulfite and bisulfite ions, Ind. Eng. Chem. Res. 29 (1990) 10–14.

[14] E. Narita, T. Sato, T. Shioya, M. Ikari, T. Okabe, Formation of hydroxylamidobis(sulfate) ion by the absorption of nitric oxide in aqueous solutions of sodium sulfite containing iron(II)-EDTA complex, Ind. Eng. Chem. Prod. Res. Dev. 23 (1984) 262–265.

[15] M.N. Ackermann, R.E. Powell, Air oxidation of hydroxylamine-*N*-sulfonate, Inorg. Chem. 6 (1967) 1718–1720.

[16] T.L. Nunes, R.E. Powell, Kinetics of the reaction of nitric oxide with sulfite, Inorg. Chem. 9 (1970) 1916–1917.

[17] D.H. Johnston, H.H. Thorp, Cyclic voltammetry studies of polynucleotide binding and oxidation by metal complexes: homogeneous electron-transfer kinetics, J. Phys. Chem. 100 (1996) 13837–13843.

[18] B. Liu, H.T. Yuan, Y.S. Zhang, Cyclic voltammetric studies of stabilized α-nickel hydroxide electrode, J. Power Sources 79 (1999) 277–280.

[19] B.E. Saltzman, Colorimetric microdetermination of nitrogen dioxide in the atmosphere, Anal. Chem. 26 (1951) 1949–1955.

[20] Z.P. Zhao, Analytical Chemistry (ch), third ed., Higher Education Press, Beijing, 1982, p. 62.

[21] H. Baralvka, Laser Raman Spectrometry Analytical Applications, Ellis Horwood Limited, 1987, pp. 1161–1166.

[22] K. Ogura, T. Ozeki, Nitrosylmetallochelates-I. Mechanism of FeNO-EDTA complex formation and its oxidation, Electrochim. Acta 26 (1981) 877–882.

[23] S.G. Chang, D. Littlejohn, N.H. Lin, Kinetics of reaction in a wet flue gas simultaneous desulfurization and denitrification system, ACS Symp. Ser. 188 (1982) 127–152.

[24] J.W. Johnson, H.W. Jiang, S.B. Hanna, W.J. James, Anodic oxidation of ethylenediamine tetraacetic acid on platinum in acid sulfate solutions, J. Eletrochem. Soc. 119 (1972) 574–580.